Polymer Vol. 38 No. 21, pp. 5347–5353, 1997
© 1997 Elsevier Science Ltd
Printed in Great Britain. All rights reserved
0032-3861/97/$17.00+0.00

PII: S0032-3861(97)00065-7

# Mechanical and thermal properties of syndiotactic polypropene filled with glass beads and talcum

**F. Stricker, M. Bruch and R. Mülhaupt***
*Freiburger Materialsforschungszentrum und Institut für Makromolekulare Chemie der Albert-Ludwigs-Universität, Stefan-Meier-Straße 21, D-79104 Freiburg i. Br., Germany*
*(Received 24 May 1996; revised 25 October 1996)*

Glass bead- and talcum-reinforced polypropene composites based on syndiotactic polypropene (s-PP) and isotactic polypropene (i-PP) were prepared to study mechanical and thermal properties and to identify influence of PP type and stereoregularity. Composites based on s-PP gave higher notched Izod impact strength than those based on i-PP, accompanied by lower Young's modulus and yield stress. The experimental Young's moduli and yield stresses of composites based on highly stereoregular s-PP and i-PP were in good agreement with theoretical predictions according to Kerner and Nicolais-Narkis, respectively. The higher relative Young's modulus and yield stress of composites based on s-PP of low stereoregularity were attributed to strong interfacial adhesion and can be described by the theory of Jancar. Lap shear tests confirmed strong glass polymer interactions. Investigations of crystallization show the nucleating effect of glass beads and talcum in the case of i-PP as well as s-PP. With increasing filler volume fraction, PP degree of crystallinity decreases. Dynamic mechanical analysis of glass bead-reinforced s-PP composites show an unexpected relaxation occurring at 55°C. © 1997 Elsevier Science Ltd.

**(Keywords: syndiotactic polypropene; composites; mechanical properties)**

## INTRODUCTION

Highly syndiotactic polypropene (s-PP) was synthesized by Ewen in 1988 by means of homogeneous metallocene-based catalysts[1]. From the point of view of industrial application, s-PP and its compounds are of less interest than isotactic polypropene (i-PP), because of its lower stiffness, although it exhibits good toughness[2]. In contrast, i-PP is used in a wide range of applications because of its attractive combination of low price, heat distortion temperature above 100°C and high stiffness.

It is common practice to lower costs and improve mechanical properties of thermoplastics by incorporating fillers. Talcum, mica and calcium carbonate are widely applied as reinforcing components[3-5]. Advantages in stiffness and dimensional stability are usually accompanied by decreased yield and ultimate strength. Poor adhesion between filler and matrix is a primary cause of low strength and poor thermomechanical properties, especially at high filler volume fractions. Because of the regular shape, glass beads are interesting for theoretical investigations, e.g. calculation of Young's modulus and tensile yield stress under consideration of interfacial adhesion[6,7].

The present paper describes the influence of glass beads and talcum on the mechanical, thermal and dynamic mechanical properties of reinforced s-PP. Composites based on s-PP of different degree of stereoregularity and i-PP are compared. Interfacial interactions were investigated by means of a lap shear test, bonding together filler and polymer. The results were compared with morphological studies of fracture surfaces, imaged by environmental scanning electron microscopy (ESEM). Aminopropyl-functionalized glass beads of 5 $\mu$m average diameter and talcum of 30 $\mu$m average diameter were blended together with PP in a twin-screw blender with counter-rotating screws at 60 rpm and 200°C for s-PP and 240°C for i-PP, respectively. Mechanical and thermal properties were studied as a function of both type and volume fraction of the filler.

## EXPERIMENTAL

### *Materials*

*Table 1* summarizes data concerning polypropene types used in this work. All polymers were commercial grades, supplied by Shell and Mitsui. Aminopropyl-functional glass beads (Potters-Ballotini 5000 CP-03, average diameter of 5 $\mu$m), containing 0.02 wt% coating of aminopropyltrimethoxysilane and talcum (Luzenac OOS, average diameter of 10 $\mu$m) were used as filler component. 0.2 wt% Irganox 1010/Irgafos 168 (4/1 wt%) were added as stabilizer during the melt processing.

### *Composite preparation*

All composites were prepared under identical mixing and moulding conditions. Filler volume fractions were varied between 0 and 30 vol%. Melt blending was performed in a Haake Rheomix 90 twin-screw kneader equipped with a 60 ml mixing chamber that was preheated at 200°C for preparation of s-PP compounds and 240°C

---

* To whom correspondence should be addressed

**Table 1** Syndiotactic and isotactic polypropene used in this study

| Polypropene | Material | rr[a] (%) | mm[a] (%) | $M_n$[b] (g mol$^{-1}$) | $M_w/M_n$ | $T_g$[c] (°C) | $T_m$[d] (°C) | Source |
|---|---|---|---|---|---|---|---|---|
| Syndiotactic | SPH-4 | 82.2 | 3.9 | 106.000 | 1.7 | 6.0 | 130 | Mitsui |
| Syndiotactic | SPH-40 | 91.1 | – | 80.000 | 1.7 | 6.1 | 132 | Mitsui |
| Isotactic | KM 6100 | – | 96.0 | 50.000 | 7.6 | 0.9 | 172 | Shell |

[a] Triads determined by $^{13}$C n.m.r.
[b] Molecular weight from g.p.c. vs polystyrene standards
[c] $T_g$ from dynamic mechanical analysis in a Rheometrics solid analyser
[d] $T_m$ determined with heating rate of 10°C min$^{-1}$ in a Perkin-Elmer DSC-7

for i-PP, respectively. Typically PP was kept together with the stabilizers, for 1.5 min at 200°C and 240°C, respectively. Then the filler was added. After 4 min total mixing time the sample was quickly recovered and quenched between metal plates. Sheets of 2 mm thickness were prepared by compression moulding in an evacuated press (Schwabenthan Polystat 100), annealing at 210 and 250°C, respectively, for 10 min and quenching to room temperature between water–cooled metal plates. Rectangular bars of a dimension of 60 mm x 10 mm x 2 mm were cut out of these plates for evaluation of mechanical properties.

### *Mechanical properties*

Tensile properties were measured on an Instron (Model 4202) tensile machine according to DIN 53455 standard procedure using test specimens of 2 mm thickness and a crosshead speed of 10 mm min$^{-1}$. Notched Izod impact strength values were determined on notched samples according to ISO 180/1A using test specimens of 60 mm x 10 mm x 2 mm. The average standard deviations of Young's modulus and yield stress were approximately 5%, of impact strength 10% and of elongation to break 30%. At least five samples were tested for each composite composition, and the average value is reported. Tests were performed at ambient temperature (23 ± 2°C) and constant humidity.

### *Thermal properties*

Thermal properties such as melting temperature, melting enthalpy, crystallization temperature and crystallization enthalpy were recorded on a Perkin-Elmer DSC-7 using a heating rate of 10 K min$^{-1}$. Prior to measurement, the samples with s-PP were heated during 5 min at 160°C, and then cooled to 105°C using a heating rate of 3 K min$^{-1}$. The samples with i-PP were heated during 5 min at 200°C and then cooled to 135°C. The annealing times at 105 and 135°C were 12 h to achieve isothermal crystallization conditions.

### *Lap shear test*

For investigations of interfacial interactions between PP and aminosilane-treated glass, thin s-PP films of approximate 0.1 mm thickness were pressed at 210°C under vacuum and cooled down rapidly to room temperature. Films of i-PP were pressed at 250°C. Two glass plates of 80 mm x 10 mm x 2 mm were washed three times with chloroform and dried under vacuum at 100°C. For aminosilane-treatment, the glass plates were heated in methanol and ammoniak (4/1) to 50°C. After adding 20 ml 3-aminopropyl-triethoxysilane per glass plate, this being in accordance with the aminosilane concentration on the surface of the glass beads, the temperature was held at 50°C for 2 h. The concentration of aminopropyl-silane on the glass plates as well as on the glass beads was too low for quantitive analysis by $HClO_4$ titration or other methods. About 350 mm$^2$ of the PP film was placed between the ends of the glass plates and pressed with 5 bar for 10 min at 150 and 200°C, respectively. The specimens were then mounted in the Instron machine. The force necessary to separate the two glass plates, was determined at crosshead speed of 1 mm min$^{-1}$. At least five specimens were measured and the average force normalized by the area of the interface to calculate the lap shear strength.

### *Dynamic mechanical analysis*

Dynamic mechanical measurements were carried out with the aid of a Rheometrics Solid Analyser RSA II and dual-cantilever geometry (frequency 1 Hz; heating rate 2 K min$^{-1}$). The sample preparation corresponds to that for mechanical investigations.

### *Electron microscopy*

The image of the matrix–filler interface was made by means of ESEM. The fracture surfaces of impact tests were investigated using an electron microscope Model 2020 of ElectroScan Corporation. The acceleration voltage was 20 kV.

## RESULTS AND DISCUSSION

### *Tensile properties*

Young's modulus and yield stress were determined for different polypropene types as a function of filler type and volume fraction. The results are illustrated in *Figures 1* and *2*. The dependence of Young's modulus on

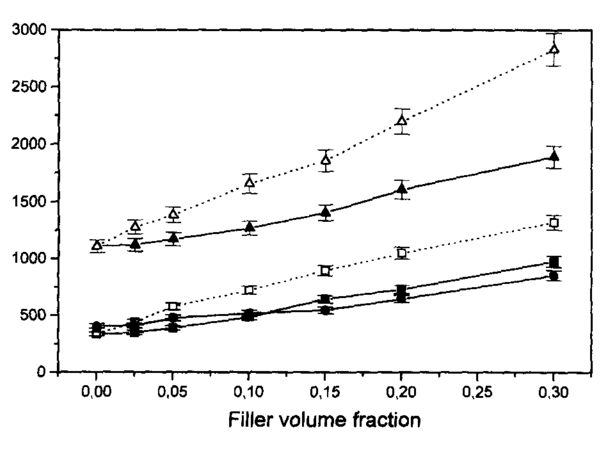

**Figure 1** Young's Modulus $E$ as a function of filler volume fraction $\phi_f$ of polypropylene composites: ■, s-PP (SPH-4) with glass beads; □, s-PP (SPH-4) with talcum; ●, s-PP (SPH-40) with glass beads; ▲, i-PP (KM 6100) with glass beads; △, i-PP (KM 6100) with talcum

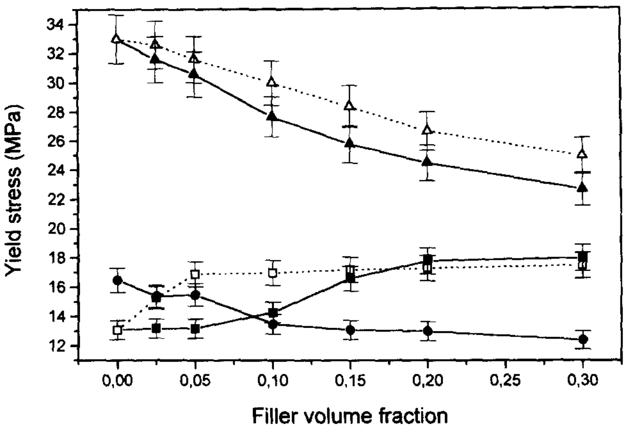

**Figure 2** Yield stress $\sigma_y$ as a function of filler volume fraction $\phi_f$ of polypropylene composites: ■, s-PP (SPH-4) with glass beads; □, s-PP (SPH-4) with talcum; ●, s-PP (SPH-40) with glass beads; ▲, i-PP (KM 6100) with glass beads; △, i-PP (KM 6100) with talcum

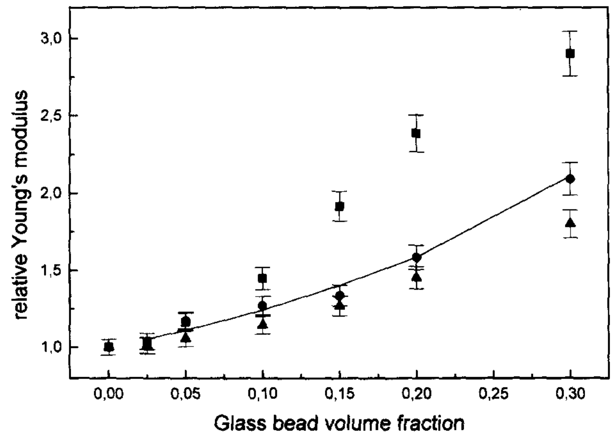

**Figure 3** Comparison of experimental data with theoretical predictions for the composite composition dependence of relative Young's Modulus $E^{\text{rel}}$: ■, s-PP (SPH-4) with glass beads; ●, s-PP (SPH-40) with glass beads; ▲, i-PP (KM 6100) with glass beads; straight line according to the equation of Kerner

filler type and volume fraction is depicted in *Figure 1*. As expected, composites moduli increase with increasing filler volume fraction. The stiffness of composites containing talcum is always higher than that of the corresponding composites containing glass beads. In general, fillers with high aspect ratio (length/diameter ratio of filler particle) show a better stiffening effect than fillers with high particle symmetry[8]. The aspect ratio of talcum[4] varies between 5 and 20, while the value of the glass beads is by definition 1. The stiffness of i-PP composites is always about three times higher than that of the corresponding composites based on s-PP.

Modulus data were compared with theoretical predictions. Several theories have been derived for composites containing spherical filler particles[9-11]. The straight line in *Figure 3* was calculated by the extended Kerner equation[12,13]:

$$E/E_m = E^{\text{rel}} = \frac{1 + A_f B_f \phi_f}{1 - B_f \Psi_f \phi_f} \tag{1}$$

where $E$ and $E_m$ are composite and polypropene moduli. $\phi_f$ is the volume fraction of the filler. According to the theory $A_f$, $B_f$ and $\Psi_f$ are expressed by equations (2), (3) and (4):

$$A_f = \frac{7 - 5\nu_m}{8 - 10\nu_m} \tag{2}$$

$$B_f = \frac{E_f - E_m}{E_f + A_f E_m} \tag{3}$$

In the equations $E_f$ is the moduli of the filler and $\nu_m$ the Poisson ratio of the polymer matrix. The Poisson ratio $\nu_{pp}$ of polypropene is taken as 0.35[13], and the moduli of glass is 69 GPa[14]. The parameter $\Psi_f$ takes into account the maximum packing fraction of the filler $\phi_f^{\max}$. In the case of random packing of single-size spheres, $\phi_f^{\max} = 0.64$[15]:

$$\Psi_f = 1 + \left[\frac{1 - \phi_f^{\max}}{\phi_f^{\max 2}}\right]\phi_f \tag{4}$$

Composites based on s-PP of high stereoregularity (SPH-40) and i-PP were in good agreement with predictions of Kerner. In contrast, the relative Young's modulus of composites based on s-PP of low stereoregularity (SPH-4) were obviously higher, though the parameters used by Kerner corresponds to the parameters of s-PP with high stereoregularity. A reason could be the influence of strong interfacial adhesion, that is not considered by Kerner. Strong interactions can cause a stiffening effect on the polymer matrix adjacent to the filler particles[6].

Yield stress, measured at large deformations, is much more dependent upon interfacial adhesion with respect to Young's modulus, measured at very small deformations. For instance, tensile yield stress proved to be an excellent property to correlate with interfacial interactions in heterogeneous polymer systems[16]. In *Figure 2* yield stress is plotted against filler volume fraction. The yield stress of composites based on i-PP decreases with increasing filler volume fraction. This is due to a smaller effective load-bearing cross-section. Again the higher aspect ratio of talcum is responsible for higher yield stresses with respect to those of glass beads. Unexpected is the behaviour of composites based on s-PP of low stereoregularity (SPH-4). The yield stress is increasing with increasing filler volume fraction, although here again the effective load-bearing cross-section is getting smaller. An explanation could be strong interfacial adhesion due to low stereoregularity of s-PP.

More information about dependence of interfacial interactions on PP type is available with the reduced yield stress plotted against filler volume fraction, as depicted in *Figure 4*. Several theories have been determined to calculate tensile yield stress[3,10,16,17]. Under assumption of low adhesion between filler and polymer matrix, a lower boundary for tensile yield stress can be obtained. Under tensile load, stress is concentrated at the equator of the particles, which decays radially, approaching the far field stress within a distance of about three particle diameters. The stress concentration depends upon the concentration of the particles, with reduction of effective matrix cross-section being the principle factor. A modified form of the equation developed by Nicolais and Narkis[17] represents a lower bound for the composite yield stress:

$$\sigma_y/\sigma_{ym} = \sigma_y^{\text{rel}} = (1 - 1.21\phi_f^{2/3})S \tag{5}$$

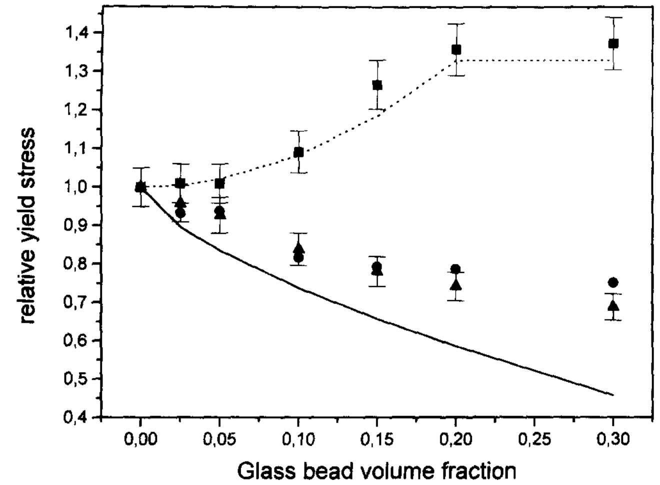

**Figure 4** Comparison of experimental data with theoretical predictions for the composite composition dependence of relative yield stress $\sigma_y^{rel}$: ■, s-PP (SPH-4) with glass beads; ●, s-PP (SPH-40) with glass beads; ▲, i-PP (KM 6100) with glass beads; dotted line according to the theory of Jancar *et al.*; straight line according to the equation of Nicolais and Narkis

where $\sigma_y$ and $\sigma_{ym}$ are the composite and matrix yield stress. The stress concentration factor $S$ can be determined by finite element analysis, and varies in general between 1.0 and 0.2, respectively, for low and high filler volume fraction. Jancar *et al.*[18] derived a model for prediction of yield stress of particulate filled thermoplastics under consideration of a random distribution of uniform size spherical particles and adhesion between filler and matrix. Under assumption of ordered cubic arrangement of the particles and zones of yielded matrix around each of adjacent particles, it is possible to define the degree of overlapping of these yielded zones. For a cubic cell to fully yield, a minimum overlap of the stress concentration field will be required, depending on filler volume fraction and interfacial adhesion. With the help of a linear elastic finite element analysis and the von Mises criterion[18] for prediction of loci of local yielding, Jancar *et al.* derived for small filler volume fractions:

$$\sigma_y/\sigma_{ym}^* = \sigma_y^{rel} = 1 + 0.33F(c)\phi_f^2 \qquad (6)$$

and for higher volume fractions:

$$\sigma_y/\sigma_{ym}^* = \sigma_y^{rel} = 1.33 \qquad (7)$$

where $\sigma_y$ is the composite yield stress and $\sigma_{ym}^*$ is the matrix yield stress in the presence of very small filler volume fraction (generally slightly less than the yield stress of the unfilled matrix). $F(c)$ is proportional to the average yielded area per particle, as characterized by the parameter $c$.

Tensile yield stresses of i-PP and s-PP composites with glass beads are shown in *Figure 4*. The modified equation of Nicolais and Narkis (equation (5)) with stress concentration fractor $S = 1$ describes the behaviour of i-PP and s-PP with high tacticity (SPH-40) reasonably well. This points to week interfacial interactions between matrix and filler. Slightly higher values of experimental results when compared with the prediction are probably caused by the polydispersity and size distribution of the glass particles.

**Table 2** Lap shear strength of PP/glass samples

| Polypropene | Lap shear strength (MPa) |
|---|---|
| s-PP (SPH-4) | 0.76 ± 0.12 |
| s-PP (SPH-40) | 0.32 ± 0.06 |
| i-PP (KM 6100) | m.n.p.[a] |

[a] m.n.p., measurement not possible

The experimental data of composites with s-PP of low stereoregularity (SPH-4) conform reasonably well with equations (6) and (7) over the whole range of volume fractions using a value of $F(c) = 25$. A comparison with experiments made by Jancar *et al.*[18] shows clearly the strong interfacial interactions between s-PP (SPH-4) and the filler. Jancar *et al.* determined for composites based on i-PP grafted with maleic anhydride and calcium-carbonate a value of $F(c) = 3.2$, only the seventh part of the value determined for s-PP (SPH-4) composites with glass beads.

A lap shear test was used to investigate macroscopic interactions between glass and PP in more detail. The lap shear strength, necessary to separate glass and a thin polymer film, reflects the interfacial adhesion and are listed in *Table 2*.

The lap shear strength, necessary to separate amino-silane-treated glass and a thin low tactic s-PP film (SPH-4), was about twice as much when compared to that of high tactic s-PP (SPH-40). This is due to the higher amorphous portion and its good adhesion to anorganic filler surface, and is in accordance with results obtained from tensile tests. The content of aminosilane on the surface of the glass plates and glass beads was too low to improve interfacial interactions significantly. It was not possible to measure the lap shear strength of specimen made of glass and i-PP, because the interactions were too weak to handle the sample.

Studies with an ESEM of fracture surfaces of PP composites containing 30 vol% glass beads are presented in *Figure 5*. Most of the fracture surface of i-PP composites is covered by glass beads (*Figure 5a*). Partially the glass beads are pulled out of the matrix, leaving craters. This is due to the weak i-PP–glass interactions. The crack propagates at the weakest part of the composites, thus at the i-PP–glass interface. In composites based on s-PP (*Figure 5b*), the interface is also the weakest part, because of the high ductility of s-PP. So the images of the fracture surfaces of s- and i-PP composites do not show a distinct difference in morphology.

### *Impact behaviour*

Notched Izod impact strength of s-PP and i-PP composites were determined as a function of filler volume fraction. In *Figure 6* notched Izod impact strength is plotted against Young's modulus with varying filler volume fraction. As expected, notched Izod impact strength of reinforced polypropene decreased with increasing filler volume fraction, whereas stiffness simultaneously increased.

Pure s-PP did not fracture in impact tests, and it took a minimum filler volume fraction to achieve fracture of the specimen at room temperature. The transition of brittle to ductile behaviour is represented in *Figure 6* by arrows. Composites based on s-PP of low stereoregularity (SPH-4) containing 5 vol% filler were still ductile, while s-PP of high tacticity (SPH-40) with only 2.5 vol% filler behaved brittly. This could be attributed

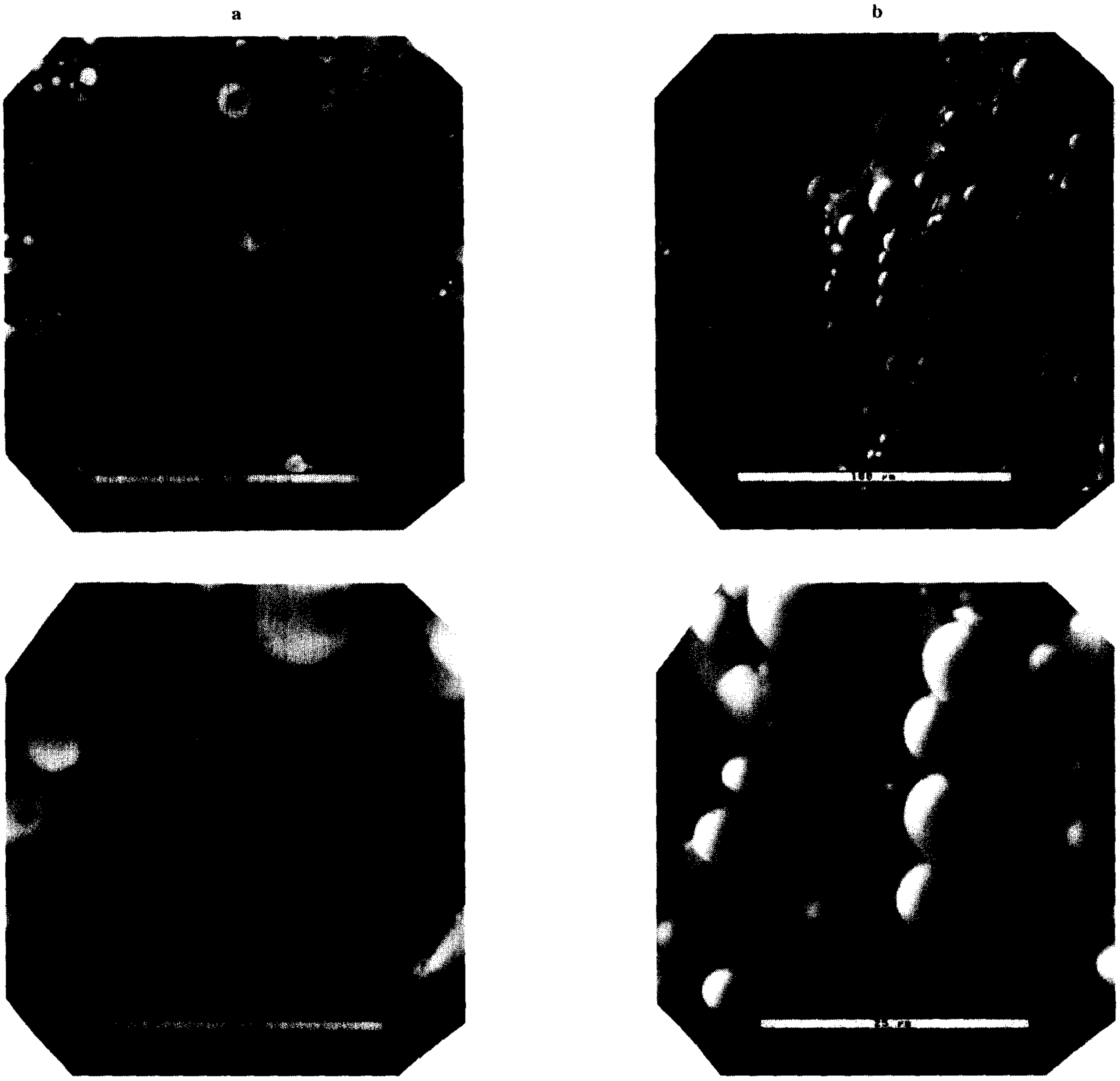

**Figure 5** ESEMs of Izod-fracture surfaces in PP composites containing 30 vol% glass beads: (a) i-PP; (b) s-PP of low tacticity (SPH-4)

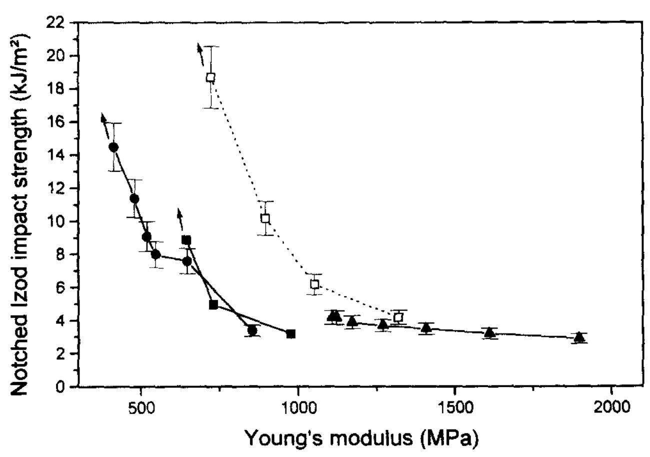

**Figure 6** Young's modulus $E$ correlated with notched Izod impact strength of polypropylene composites containing different filler volume fractions, which varies from right to left from 30 to 20, 15, 10, 5, 2.5, 0 vol%: ■, s-PP (SPH-4) with glass beads; □, s-PP (SPH-4) with talcum; ●, s-PP (SPH-40) with glass beads; ▲, i-PP (KM 6100) with glass beads. The arrows indicate the transition from ductile to brittle behaviour; with less filler volume fraction the samples did not break

to differences in degree of stereoregularity, accompanied by differences in degree of crystallinity. There is no significant difference in impact behaviour between composites with glass beads and talcum. *Figure 6* clearly shows the advantage of talcum with respect to glass beads concerning stiffness–impact behaviour.

### *Thermal properties*

Thermal properties of filled composites based on i-PP are already well investigated and discussed elsewhere[19–21]. Melt and crystallization behaviour of s-PP composites were determined as a function of filler type and volume fraction and compared with thermal properties of composites based on i-PP. The results are listed in *Table 3*.

In general, s-PP crystallizes at lower temperatures than i-PP. After slow cooling of molten s-PP, it forms needles while i-PP crystallizes as spherulites[22]. Glass beads and talcum were nucleating s-PP as well as i-PP. This was monitored by means of differential scanning calorimetry (d.s.c.). Talcum in i-PP exhibited a higher nucleating activity than glass beads. This nucleating effect was also observed in s-PP and is reflected by higher crystallization

**Table 3** Thermal properties of s-PP and i-PP composites with glass beads and talcum

| Polypropene | Glass beads (vol%) | Talcum (vol%) | $T_{\mathrm{cryst.}}$ (°C) | $\Delta H_{\mathrm{cryst.}}$ ($\mathrm{J\,g^{-1}}$) | $T_{\mathrm{m}}$ (°C) | $\Delta H_{\mathrm{m}}$ ($\mathrm{J\,g^{-1}}$) |
|---|---|---|---|---|---|---|
| s-PP (SPH-4) | 0 | / | 69.1 | −29.8 | 129.7 | 39.4 |
| | 5 | / | 71.5 | −28.6 | 129.7 | 39.3 |
| | 10 | / | 71.8 | −28.2 | 129.2 | 39.0 |
| | 20 | / | 72.8 | −26.6 | 129.4 | 37.3 |
| | 30 | / | 73.6 | −26.4 | 128.8 | 37.3 |
| | / | 5 | 82.7 | −23.7 | 131.1 | 34.6 |
| | / | 10 | 83.7 | −22.4 | 130.7 | 34.5 |
| | / | 20 | 86.1 | −17.9 | 130.6 | 33.9 |
| | / | 30 | 88.1 | −15.7 | 128.7 | 33.5 |
| s-PP (SPH-40) | 0 | / | 76.1 | −26.7 | 131.9 | 34.6 |
| | 5 | / | 77.9 | −26.2 | 132.0 | 34.0 |
| | 10 | / | 77.9 | −26.3 | 132.5 | 34.0 |
| | 20 | / | 78.0 | −25.8 | 131.8 | 33.5 |
| | 30 | / | 78.4 | −25.3 | 130.9 | 33.4 |
| i-PP (KM 6100) | 0 | / | 108.6 | −93.3 | 171.1 | 105.8 |
| | 5 | / | 112.5 | −93.2 | 171.4 | 104.5 |
| | 10 | / | 114.0 | −92.5 | 171.2 | 104.3 |
| | 20 | / | 114.4 | −91.5 | 170.5 | 102.0 |
| | 30 | / | 115.8 | −91.0 | 171.0 | 98.1 |
| | / | 5 | 120.3 | −93.2 | 169.4 | 104.6 |
| | / | 10 | 121.8 | −92.2 | 169.8 | 104.5 |
| | / | 20 | 123.8 | −89.6 | 168.9 | 102.9 |
| | / | 30 | 124.7 | −89.1 | 169.3 | 101.6 |

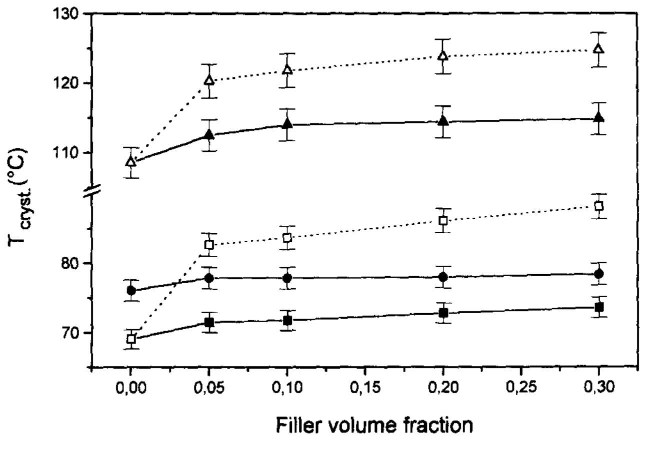

**Figure 7** Crystallization temperature $T_{\mathrm{cryst.}}$ as a function of filler volume fraction $\phi_{\mathrm{f}}$: ■, s-PP (SPH-4) with glass beads; □, s-PP (SPH-4) with talcum; ●, s-PP (SPH-40) with glass beads; ▲, i-PP (KM 6100) with glass beads; △, i-PP (KM 6100) with talcum

temperatures $T_{\mathrm{cryst}}$ when cooling down molten PP composites, as shown in *Figure 7*.

As listed in *Table 3*, melt and crystallization enthalpy, $\Delta H_{\mathrm{m}}$ and $\Delta H_{\mathrm{cryst}}$, and consequently the degree of crystallinity, decreased with increasing filler volume fraction. A consequence of nucleation is a larger number of small i-PP spherulites or s-PP needles and an increased impingement area between the spherulites or needles. Because of the lower crystallinity of the impingement area, the degree of crystallinity of s-PP and i-PP composites is decreasing with increasing filler volume fraction. Under the assumption of similar melt enthalpies of 100% crystallines-PP and i-PP, the degree of crystallinity of i-PP is about three to four times that of s-PP. This is a main reason for higher notched Izod impact strength and lower stiffness of s-PP and its composites with respect to i-PP. It should be mentioned, that polydispersity and especially stereoregularity influence crystallization behaviour. As seen in *Table 1*, the types of s-PP used have a narrow distribution of molecular weight and a lower stereoregularity, when compared to i-PP. Beside the lower tendency of s-PP to crystallize, lower stereoregularity of s-PP is a reason for a reduced degree of crystallinity with respect to i-PP. The melting point $T_{\mathrm{m}}$ of the composites is almost unaffected by the addition of fillers.

### *Dynamic mechanical properties*

The dynamic mechanical properties of filled i-PP are already intensively investigated[7,23,24]. Temperature dependences of loss factor tan $\delta$ of s-PP composites with glass beads are shown in *Figure 8*. The loss factor peak located at about 6°C corresponds to the glass transition of s-PP, detected at a frequency of about 1 Hz. The glass transition temperature ($T_{\mathrm{g}}$) is almost unaffected by filler volume fraction. The loss factor tan $\delta$ of s-PP composites containing 10 and more vol% glass beads show an unexpected peak at about 55°C. With increasing glass bead volume fraction the area under the peak is growing and the loss factor below the peak has higher values.

The peak should result from relaxation processes occurring at the s-PP–glass interface, because pure s-PP does not show this effect. An immobile phase around the filler particle should lead to a shift of $T_{\mathrm{g}}$, as predicted by Howard and Shanks[25]. However the observed peak shift is too large to be explained by immobilization of the matrix around the filler particle. Besides talcum should

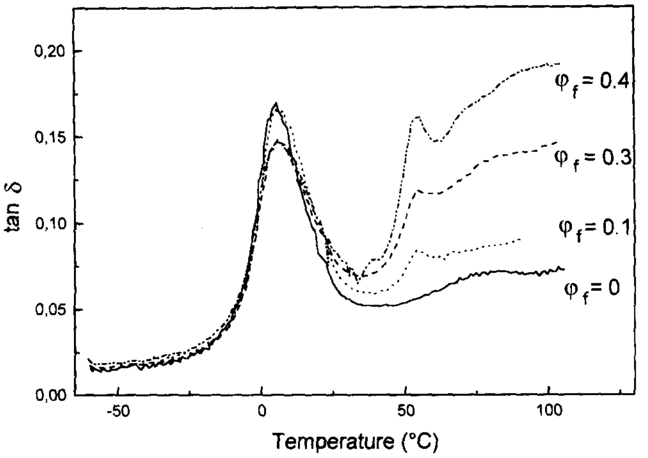

**Figure 8** Temperature dependence of tan $\delta$ of polypropylene composites with different glass bead volume fractions $\phi_f$

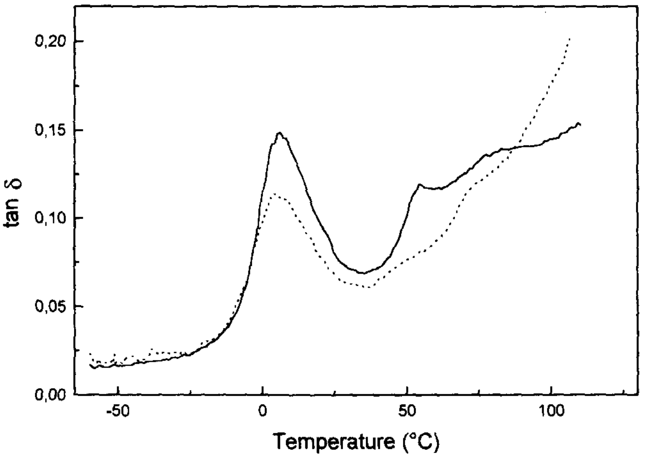

**Figure 9** Temperature dependence of tan $\delta$ of polypropylene composites with 30 vol% glass beads (straight line) and with 30 vol% talcum (dotted line)

cause the same effect, but as shown in *Figure 9*, s-PP composites containing 10 vol% talcum do not have an equivalent peak.

## CONCLUSION

The influence of filler volume fraction on mechanical properties of PP composites as well as on fracture surface aspects indicate strong interfacial adhesion between low stereoregular s-PP and anorganic fillers with respect to highly stereoregular s-PP and i-PP. The moduli of composites based on highly stereoregular s-PP and i-PP were in good agreement with the predictions of Kerner, while filled s-PP with lower stereoregularity has higher values. Talcum in s-PP as well as i-PP gave higher stiffness with respect to glass beads. Analysis of tensile yield stress and lap shear tests indicated good glass–PP adhesion in composites containing low stereoregular s-PP and glass beads, as described by the theory of Jancar *et al.* Weaker adhesion was determined for composites based on highly stereoregular s-PP and i-PP. The results are in accordance with predictions by Nicolais and Narkis. These effects are attributed to good adhesion between atactic, amorph polymer regions and the anorganic filler surface. Fracture surface analysis by means of ESEM did not reveal features typical for improved adhesion. The notched Izod impact strength of s-PP and its composites was much higher than those of i-PP. Moreover, notched Izod impact strength was almost independent of filler type. By means of d.s.c. it was possible to demonstrate the nucleating effect of glass beads and talcum on s-PP and i-PP, with talcum being the more efficient nucleating agent. Comparison of melt enthalpies reflected much lower degree of crystallinity of s-PP and its composites with respect to those of i-PP. This accounts for the higher stiffness and lower impact strength of i-PP and its composites when compared with s-PP.

## ACKNOWLEDGEMENT

The authors would like to thank Shell Research in Louvain-la-Neuve-Belgium, in particular A. Wirtz and A. Farina, for supporting this study.

## REFERENCES

1. Ewen, J. A., Jones, R. L., Razavi, A. and Ferrara, J. D., *J. Am. Chem. Soc.*, 1988, **110**, 6255.
2. Setz, S., Stricker, F., Kressler, J., Duschek, T. and Mülhaupt, R., *J. Appl. Polym. Sci.*, 1996, **59**, 1117.
3. Maiti, S. N. and Sharma, K. K., *J. Mater. Sci.*, 1992, **27**, 4605.
4. Asmus, K. D., *Kunststoffe*, 1980, **70**, 336.
5. Schlumpf, H. P., *Kunststoffe*, 1987, **77**, 1092.
6. Shang, S. W., Williams, J. W. and Söderholm, K. J. M., *J. Mater. Sci.*, 1994, **29**, 2406.
7. Lee, B.-L. and Nielsen, L. E., *J. Polym. Sci., Polym. Phys. Edn*, 1977, **15**, 683.
8. Chow, T. S., *J. Polym. Sci., Polym. Phys. Edn*, 1978, **16**, 959.
9. Takayanagi, M., Uemura, S. and Minami, S., *J. Polym. Sci.*, 1994, **5C**, 113.
10. Ahmed, S. and Jones, F. R., *J. Mater. Sci.*, 1990, **15**, 4933.
11. Theocaris, P. S. and Sideridis, E., *J. Appl. Polym. Sci.*, 1984, **29**, 2997.
12. Kerner, E. H., *Proc. Phys. Soc.*, 1956, **69B**, 808.
13. Chiang, W. Y., Yang, W. D. and Pukanszky, B., *Polym. Eng. Sci.*, 1992, **32**, 641.
14. Elias, H.-G., Makromoleküle, Huthig & Wepf Verlag, 1990.
15. Kolarik, J. and Jancar, J., *Polymer*, 1992, **33**, 4961.
16. Pukanszky, B., *Composites*, 1990, **21**, 255.
17. Nicolais, L. and Narkis, M., *Polym. Eng. Sci.*, 1971, **11**, 194.
18. Jancar, J., Dianselmo, A. and Dibenedetto, A. T., *Polym. Eng. Sci.*, 1992, **32**, 1394.
19. Kowalewski, T. and Galeski, A., *J. Appl. Polym. Sci.*, 1986, **32**, 2919.
20. Menczel, J. and Varga, J., *J. Therm. Analysis*, 1983, **28**, 161.
21. McGenity, P. M., Hooper, J. J., Paynter, C. D., Riley, A. M., Nutbeem, C., Elton, N. J. and Adams, J. M., *Polymer*, 1992, **33**, 5215.
22. Thomann, R., Wang, C., Kressler, J., Jüngling, S. and Mülhaupt, R., *Polymer*, 1995, **36**, 3795.
23. Sumita, M., Tsukihi, H., Miyasaka, K. and Ishikana, K., *J. Appl. Polym. Sci.*, 1984, **29**, 1523.
24. Theocaris, P. S., *Colloid Polym. Sci.*, 1987, **265**, 461.
25. Howard, G. J. and Shanks, R. A., *J. Appl. Polym. Sci.*, 1981, **26**, 3099.